Toward an Understanding of the High Enantioselectivity in the Osmium-Catalyzed Asymmetric Dihydroxylation. 3. New Insights into Isomeric Forms of the Putative Osmaoxetane Intermediate

Per-Ola Norrby,[†] Heinrich Becker,[‡] and K. Barry Sharpless*[,‡]

Contribution from the Royal Danish School of Pharmacy, Department of Medicinal Chemistry, Universitetsparken 2, DK-2100 Copenhagen, Denmark, and Department of Chemistry, The Scripps Research Institute, 10666 N. Torrey Pines Road, La Jolla, California 92037

Received July 24, 1995[⊗]

Abstract: A systematic study of the possible diastereomeric osmaoxetane intermediates in the asymmetric dihydroxylation reaction (AD) has been undertaken. Several of these intermediates have been examined by DFT-calculations using ruthenium as a model for osmium. Changes in the puckering of the metallaoxetane, together with interactions of the substrate with the "binding pocket" of the ligand, seem to be responsible for the selectivities observed for the different olefin substitution patterns. Two levels of enantioselection, formation of the ligated osmaoxetane *and* its rearrangement to the glycolate, add up to the usually observed high enantioselectivity. An electrostatic dipole−dipole interaction between the osmaoxetane and the ester/imino ester moiety of the ligand is proposed to play an additional role in the transition state stabilization. The osmaoxetane intermediate explains all observed enantioselectivities in the asymmetric dihydroxylation reaction.

The oxidation of olefins with osmium tetraoxide is probably both the most general and most selective organic reaction known to date: osmium tetraoxide reacts with almost *all olefins*, it is an *extremely mild* oxidizing agent, and it tolerates *almost every* other organic functional group. This statement describing the reagents scope, reactivity, and selectivity seems to demand mutually exclusive properties. Great scope and high selectivity are usually found at the extremes of the reactivity spectrum, but in osmium tetraoxide's reactions with olefins they coexist. The secret of course resides in the mechanism and specifically in the gentle[1] but ineluctable sequence by which the two oxygens are transferred from osmium to olefin. The recent development of osmium-catalyzed asymmetric dihydroxylation (the AD reaction, Figure 1)[2] has rekindled interest in the mechanism. Two major pathways, with several variations, have been proposed for the dihydroxylation process: A concerted [3 + 2] cycloaddition,[3] and a formal [2 + 2] cycloaddition[4] leading to an osmaoxetane intermediate which in turn rearranges to the primary product, the osmium(VI) glycolate.[5]

We have recently shown that part of the explanation for this high enantioselectivity is the presence of at least two selectivity-determining levels in the reaction.[6] For several different olefin and ligand combinations the AD process exhibited a nonlinear temperature−enantioselectivity relationship,[6] strongly indicating the presence of an intermediate on the reaction pathway. Furthermore, it is required that the transition states leading to and from this intermediate have unequal temperature dependencies and equal free energies at the inversion temperature (usually between −20 °C and +10 °C) (Figure 2).[7] These facts do not support a concerted [3 + 2] mechanism. On the other hand, the osmaoxetane intermediate postulated in the formal [2 + 2] mechanism can explain the observed behavior. Such metallaoxetane species have been shown to be plausible intermediates by quantum chemical calculations.[4d,8] The Hammond postulate states that these high energy species are close to the selectivity-determining transition state in the reaction.

[†] Royal Danish School of Pharmacy.

[‡] The Scripps Research Institute.

[⊗] Abstract published in *Advance ACS Abstracts,* December 1, 1995.

(1) $\Delta G^{\ddagger}$ is usually between 5 and 7 kcal/mol. (a) Kwong, H.-L. Ph.D. Thesis, Massachusetts Institute of Technology, 1993. (b) Nelson, D. W.; Sharpless, K. B. Unpublished results.

(2) (a) Sharpless, K. B.; Amberg, W.; Bennani, Y. L.; Crispino, G. A.; Hartung, J.; Jeong, K.-S.; Kwong, H.-L.; Morikawa, K.; Wang, Z.-M.; Xu, D.; Zhang, X.-L. *J. Org. Chem.* **1992**, *57*, 2768 and references cited therein. (b) Crispino, G. A.; Jeong, K.-S.; Kolb, H. C.; Wang, Z.-M.; Xu, D.; Sharpless, K. B. *J. Org. Chem.* **1993**, *58*, 3785. (c) Sharpless, K. B.; Amberg, W.; Beller, M.; Chen, H.; Hartung, J.; Kawanami, Y.; Lübben, D.; Manoury, E.; Ogino, Y.; Shibata, T.; Ukita, T. *J. Org. Chem.* **1991**, *56*, 4585. For reviews, see: (d) Lohray, B. B. *Tetrahedron: Asymmetry* **1992**, *3*, 1317. (e) Johnson, R. A.; Sharpless, K. B. Catalytic Asymmetric Dihdyroxylation. In *Catalytic Asymmetric Synthesis*; Ojima, I., Ed.; VCH: Weinheim, 1993; pp 227−272. (f) Kolb, H. C.; VanNieuwenhze, M. S.; Sharpless, K. B. *Chem. Rev.* **1994**, *94*, 2483.

(3) (a) Böseken, J. *Rec. Trav. Chim.* **1992**, *41*, 199. (b) Criegee, R. *Justus Liebig Ann. Chem.* **1936**, *75*, 522. (c) Criegee, R. *Angew. Chem.* **1937**, *50*, 153. (d) Criegee, R. *Angew. Chem.* **1938**, *51*, 519. (e) Criegee, R.; Marchand, B.; Wannowias, H. *Justus Liebig Ann. Chem.* **1942**, *99*, 550. (f) Jørgensen, K. A.; Hoffmann, R. *J. Am. Chem. Soc.* **1986**, *108*, 1867. (g) Herrmann, W. A.; Eder, S. J.; Scherer, W. *Angew. Chem., Int. Ed. Engl.* **1992**, *31*, 1345. (h) Lohray, B. B.; Bhushan, V. *Tetrahedron Lett.* **1992**, *33*, 5113. (i) Lohray, B. B.; Bhushan, V. *Tetrahedron Lett.* **1993**, *34*, 3911. (j) Corey, E. J.; Noe, M. C.; Sarshar, S. *J. Am. Chem. Soc.* **1993**, *115*, 3828. (k) Corey, E. J.; Noe, M. C. *J. Am. Chem. Soc.* **1993**, *115*, 12579. (l) Corey, E. J.; Noe, M. C.; Sarshar, S. *Tetrahedron Lett.* **1994**, *35*, 2861. (m) Corey, E. J.; Noe, M. C.; Grogan, M. J. *Tetrahedron Lett.* **1994**, *35*, 6427. (n) Corey, E. J.; Guzman-Perez, A.; Noe, M. C. *J. Am. Chem. Soc.* **1994**, *116*, 12109.

(4) (a) Sharpless, K. B.; Teranishi, A. Y.; Bäckvall, J.-E. *J. Am. Chem. Soc.* **1977**, *99*, 3120. (b) Hentges, S. G.; Sharpless, K. B. *J. Am. Chem. Soc.* **1980**, *102*, 4263. (c) Jørgensen, K. A.; Schiøtt, B. *Chem. Rev.* **1990**, *90*, 1483−1506. (d) Norrby, P.-O.; Kolb, H. C.; Sharpless, K. B. *Organometallics* **1994**, *13*, 344. (e) Norrby, P.-O.; Kolb, H. C.; Sharpless, K. B. *J. Am. Chem. Soc.* **1994**, *116*, 8470. (f) Lohray, B. B.; Bhushan, V.; Nandanan, E. *Tetrahedron Lett.* **1994**, *35*, 4209. (g) Becker, H.; Ho, P. T.; Kolb, H. C.; Loren, S.; Norrby, P.-O.; Sharpless, K. B. *Tetrahedron Lett.* **1994**, *35*, 7315.

(5) Pearlstein, R. M.; Blackburn, B. K.; Davis, W. M.; Sharpless, K. B. *Angew. Chem., Int. Ed. Engl.* **1990**, *29*, 639.

(6) (a) Göbel, T.; Sharpless, K. B. *Angew. Chem., Int. Ed. Engl.* **1993**, *32*, 1329. (b) Commentary on 6a: Brückner, C.; Dolphin, D. *Chemtracts* **1993**, *6*, 364.

(7) Buschmann, H.; Scharf, H.-D.; Hoffmann, N.; Esser, P. *Angew. Chem., Int. Ed. Engl.* **1991**, *30*, 477.

(8) Veldkamp, A.; Frenking, G. *J. Am. Chem. Soc.* **1994**, *116*, 4937.

0002-7863/96/1518-0035$12.00/0

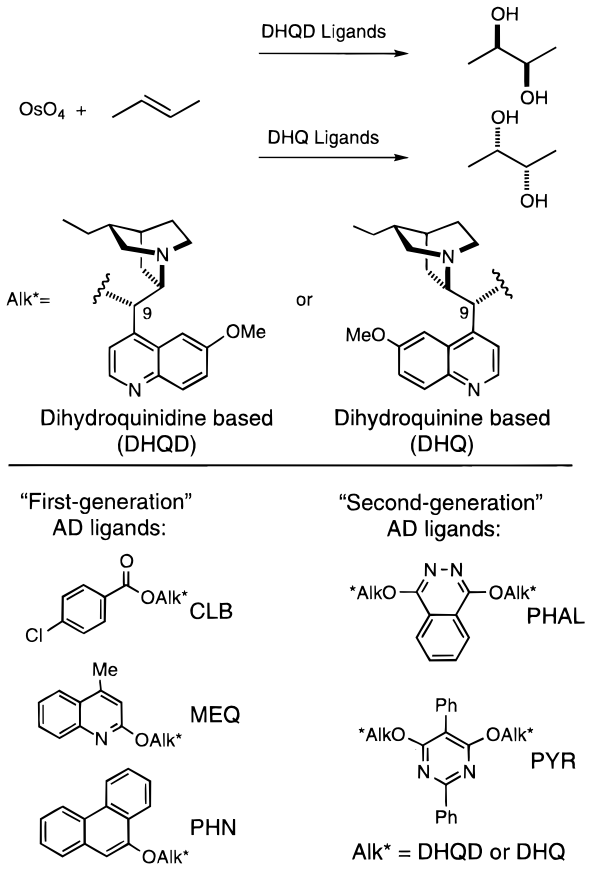

Figure 1. The AD reaction.

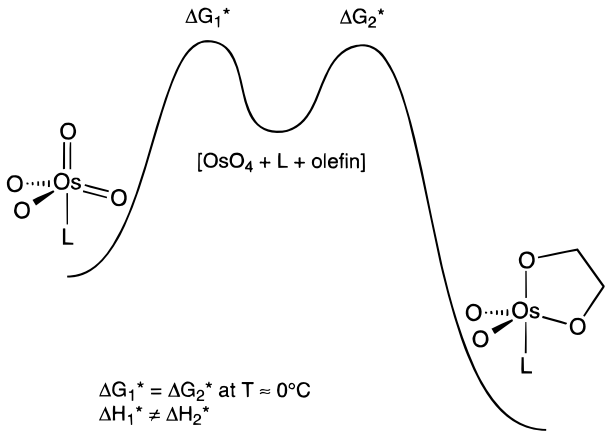

Figure 2. The simplest possible reaction path for the AD reaction (L = amine ligand).

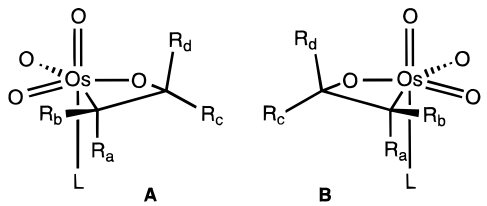

Figure 3. Two isomeric models of osmaoxetane ligand complexes with substituent labels (enantiomeric if ligand L is achiral, diastereomeric if L is chiral).

We have recently shown that many features of the reaction can be rationalized by a molecular mechanics model of the osmaoxetane intermediate.[4e] To the best of our knowledge, a reaction path including an osmaoxetane ligand complex (Figure 3) is the only proposed mechanism for the AD reaction that is consistent with all the observations made to date.[6]

The presence of (at least) *two* selectivity-determining steps in the osmylation may also be a reason for the extraordinarily high enantioselectivity usually observed in the AD reaction (for *trans*-1,2-di- and trisubstituted olefins an ee of >95% is usually obtained, even if the olefin is only alkyl substituted). If the energies of the transition states leading to (ΔG_1*) and from (ΔG_2*) the intermediate are effected in the same way by a chiral ligand, *amplification* of the selectivity should take place.

It is possible to envision several reaction pathways through the intermediate **A/B**. We favor the mechanism depicted in Figure 4. The most obvious advantage of this mechanism over alternative [2 + 2] proposals is that each step leading up to the intermediate **A/B** has chemical precedent. Steps 1, 2, and 4 are simple ligand exchange equilibria. Step 3 involves rapid equilibrium between an olefin d^0 metal−oxo-complex and the corresponding metallaoxetane. Analogous equilibria are known to be very fast for olefin complexes of d^0 metal−imido (M═NR) and metal−ylide (M═CHR) species.[9] An alternative mechanism that would still display the same kinetic behavior is direct [2 + 2] addition of an olefin to a ligand−osmium tetroxide complex.[4f,10] However, such a direct addition to an 18-electron complex is unprecedented.

Our tentative molecular mechanics model[4e] has been successful in rationalizing selectivities for a wide range of substrates. The puckering of the osmaoxetane ring, putting two of the substituents into pseudoequatorial positions, turns out to have great influence on the expected selectivity.[4d,11] However, the effects of different substitution patterns were not specifically evaluated. Therefore, we report here analyses of the selectivity-determining interactions in the osmaoxetane ligand complex, based on both DFT (density functional theory) calculations and experimental results. The studies also provide a basis for refinement of the molecular mechanics model and demonstrate the use of the current parameter set as a tool in quantitative selectivity predictions.

DFT Calculations. We have previously reported DFT calculations on the ruthenium analog of **A/B** with an unsubstituted metallaoxetane ring.[4d] It was assumed that steric parameters would be similar in the corresponding osmium and ruthenium complexes, and later *ab initio* calculations on **A/B** using an Os ECP basis set indeed yielded structures very similar to our results.[8] We have also shown that other Ru(VIII) and Ru(VI) structures calculated by DFT agree closely with X-ray structures of the corresponding Os complexes,[4d] and it has been established that RuO_4 dihydroxylations[12] in the presence of AD ligands give the same enantiofacial selectivities as OsO_4 dihydroxylations, albeit with lower yield and selectivity.[13] It was therefore assumed that the DFT calculations on ruthenaoxetane ligand complexes, if interpreted cautiously, might yield information about trends in the interaction between substituents on the oxetane and the ligand in the corresponding osmaoxetane ligand complexes. The calculated complexes are shown in Figure 5. Some isodesmic[14] energy differences are shown in Table 1.

(9) (a) Meyer, K. E.; Walsh, P. J.; Bergman, R. G. *J. Am. Chem. Soc.* **1994**, *116*, 2669. (b) de With, J.; Horton, A. D.; Orpen, A. G. *Organometallics* **1993**, *12*, 1493. (c) Bennett, J. L.; Wolczanski, P. T. *J. Am. Chem. Soc.* **1994**, *116*, 2179.

(10) Norrby, P.-O.; Gable, K. P. *J. Chem. Soc., Perkin Trans. 2*, in press.

(11) Puckering is proposed to play a key role in the extrusion of alkenes from rhenium(V) diolates, which is essentially the microscopic reverse of the osmylation process: (a) Gable, K. P.; Juliette, J. J. J. *J. Am. Chem. Soc.* **1995**, *117*, 955. (b) Gable, K. P. Personal communication.

(12) (a) Footnote 3 in: Sharpless, K. B.; Akashi, K. *J. Am. Chem. Soc.* **1976**, *98*, 1986. (b) Shing, T. K. M.; Tai, V. W.-F.; Tam, E. K. W. *Angew. Chem., Int. Ed. Engl.* **1994**, *33*, 2312.

(13) Xu, D.; Sharpless, K. B. Unpublished results.

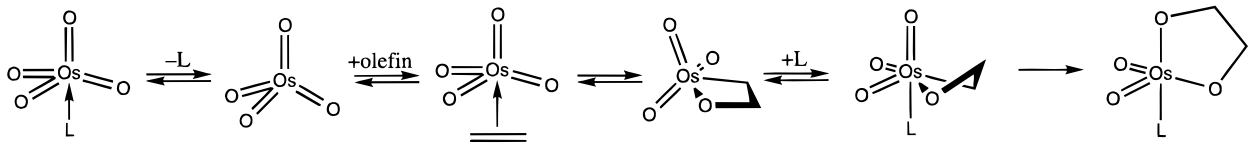

Figure 4. The currently most viable proposal for the [2 + 2] mechanism.

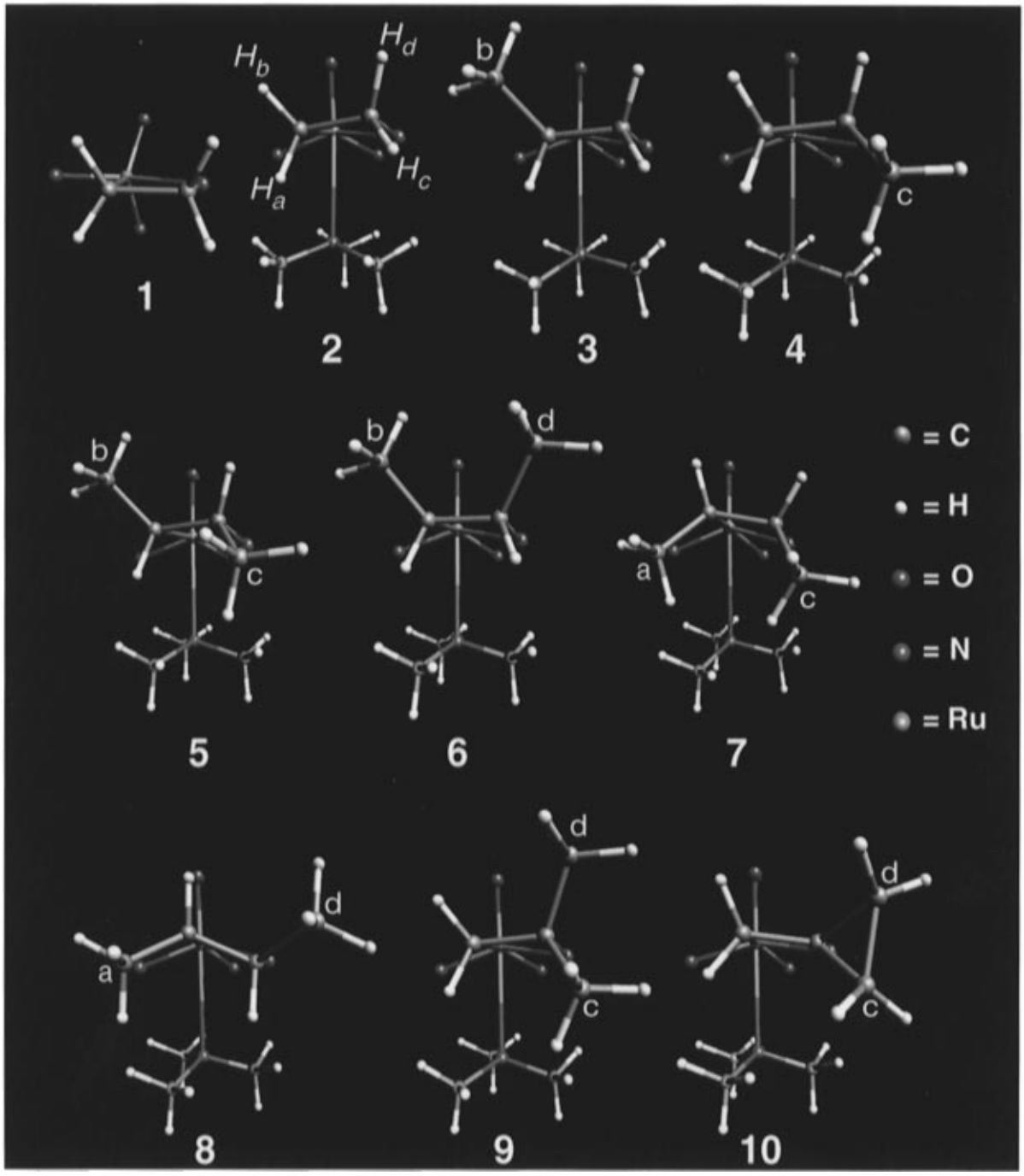

Figure 5. Calculated metallaoxetane ligand complexes. M = Ru in the calculations, M = Os in the AD reaction. Unsubstituted and unligated oxetane **1**[4d] has been calculated earlier; it exhibits no puckering.

All complexes are fully optimized. No substituents larger than methyl could be systematically investigated at this level of theory (of course, steric effects will be larger with almost any other substituent).

Comparing first the two pseudoequatorial positions **b** and **c** (monosubstituted complexes **3** and **4**), we find that occupancy of position **c** is more favorable due to less crowding (**4** is more stable than **3**). Compared to the unsubstituted complex **2**, we

Table 1. Calculated Isodesmic Energy Differences in kJ/mol

	ΔE		ΔE		ΔE
3−**4**	4[a]	**6**−**5**	5	**7**−**5**	21
8−**5**	15	**9**−**5**	7[a]		

[a] Change in connectivity, more uncertain value.

(14) Isodesmic comparisons are expected to give reliable results even at fairly low levels of theory: Hehre, W. J.; Radom, L.; Schleyer, P. v. R.; Pople, J. A., *Ab Initio Molecular Orbital Theory*; Wiley: New York, 1986.

Chart 1. Influence of the Substitution Pattern of Aliphatic Olefins on the Rate of the Dihydroxylation.[15] All Rates are Measured in *t*-BuOH/H_2O 6:1 (the same ratio as in the organic phase in the catalytic AD) at 0 °C; the Concentration of Ligand and Olefin are 0.04 mol/L.

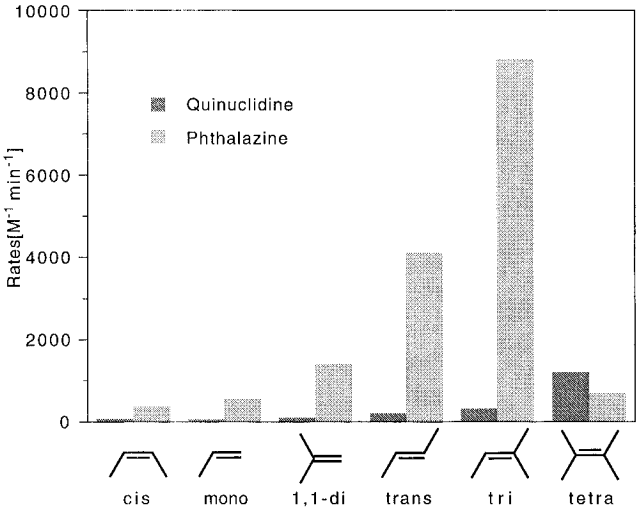

also see that a substituent in position **b** wants to be staggered with the two proximal oxo groups, leading to a reduction in the puckering of the ring. A **c**-substituent, on the other hand, increases the puckering by seeking a more equatorial position. These two effects are not additive: the **b**,**c**-disubstituted oxetane **5** actually has the highest puckering of all calculated complexes. The favoring of **c** over **b** may be within the error limits of our methods and will definitely be altered by substituents more complex than methyl (e.g., phenyl).

Of the calculated disubstituted complexes (**5** → **10**), **5** has the lowest energy and the highest degree of puckering. Moving the **c** substituent to position **d** results in complex **6** which has a slightly higher energy and exhibits much less puckering. Complexes **5** and **6** are the preferred intermediates resulting from *trans*- and *cis*-1,2-disubstituted olefins, respectively. Complex **7**, the alternative isomer for *cis*-olefins, has a much higher energy. The M−N bond in **7** is drastically elongated, to the point where the amine no longer coordinates significantly to the metal center. This is in accord with our molecular mechanics study,[4e] where it was concluded that the substituent in position **a** in a ligated metallaoxetane must be hydrogen. For the case where this position **must** be occupied by a group larger than hydrogen, that is, tetrasubstituted olefins, it is doubtful whether the ligated metallaoxetane can be considered a true intermediate. In tetrasubstituted metallaoxetane complexes without a ligand, this position is not very crowded,[4d] but an incoming strongly binding ligand should force synchronous rearrangement to the observed product. In the absence of a true ligated metallaoxetane intermediate, nonbonded interactions between the ligand and the olefinic moiety will not be fully developed and this could partly rationalize the lower enantioselectivities observed for most members of this olefin class. It has also been shown that for the very strong ligand quinuclidine, tetrasubstituted olefins exhibit the highest rates of the six olefin classes, whereas with the much weaker binding *cinchona* ligands, tetrasubstituted olefins are nearly the least reactive of the six olefin classes (Chart 1).[15]

Complex **8** which is the alternative isomer for *trans*-olefins also has a high energy. The calculated energy difference between **8** and **5** is about 15 kJ/mol. Complex **8** is interesting in that it is the only isomer for which we have obtained an oxetane ring where the puckering is actually reversed (the four-membered ring has been flipped, making positions **a** and **d** pseudoequatorial). We have previously suggested that such an intermediate could be a contributor to minor enantiomer generation in the dihydroxylation of monosubstituted olefins.[4e] Attempts to locate a reversed puckering conformation on the energy hypersurface of the **d**-monosubstituted oxetane (not shown in Figure 5) have failed. However, the energies of reversed puckered geometries are probably within the uncertainty limit of our methods. From these calculations, we cannot conclude whether a "reverse puckered" oxetane can exist for monosubstituted olefins or not. This question has to be addressed by analyzing experimental selectivities (*vide infra*).

The effect of a **d**-substituent can also be seen in complex **9**, the intermediate resulting from a 1,1-disubstituted olefin. The energy is calculated to be slightly higher than for either complex **5** or **6**, but since the connectivity has changed, this result may be an artifact of the method. The puckering is lower than for the **c**-monosubstituted complex **4**, as expected from the repulsive "diaxial" interaction with the axial oxo group. However, the puckering is still larger than for complex **6**, where the two groups **b** and **d** both reduce the puckering.

Complex **10** represents intermediates obtained from highly strained olefins (in this case methylene cyclopropane). It can formally be considered an analog of complex **9**, as it is 1,1-disubstituted. However, the strain energy from the spiro-annulation of the three-membered ring results in an oxetane that is almost completely flat. For all other complexes in this study, the M−C−C−O torsional angle lies between 10° and 20°, whereas in complex **10** this angle is <3°. It also has the shortest M−N bond in this study, probably due to a lowered repulsion between H_a and the amine ligand.

To summarize the puckering, the preferred complexes for the different disubstituted olefins show the trend **5** > **9** > **6**. Intriguingly, this trend correlates both with the relative rates of dihydroxylation[15] (Chart 1) and the observed enantioselectivities[2e,f] for these olefin classes (*cf.* Table 2).

Due to the approximations made in these calculations, it is not appropriate to draw conclusions about preferred isomeric intermediates from the calculated energies, except to note the strong crowding of position **a**. In addition, we feel it is reasonable to use the calculated geometrical trends as an aid for extracting information about the possible isomeric intermediates from available experimental data (*vide infra*).

Oxetanes in the Presence of a Chiral Ligand. The interactions between *cinchona*-derived ligands and the oxetane moiety of the complex have been investigated by molecular mechanics methods.[4e] The calculations reveal the steric crowding of position **a** mentioned previously. It has already been shown that the binding constant for quinuclidine derivatives to OsO_4 is extremely sensitive to steric effects. The binding constant of quinuclidine to OsO_4 in *t*-BuOH at 25 °C is 2630 L/mol; the binding constant of $(DHQD)_2$-PHAL is only 27.7 L/mol under the same conditions.[16] This dramatic effect also suggests that crowding of position **a** *in the oxetane* is much stronger with the AD-ligands than with quinuclidine.

The following discussion will center on DHQD-based ligands, for which intermediate **A** was shown to be favored over its diastereomer **B** due to nonbonded attractive stabilization of substituents in position **c**. The importance of the attractive stabilization can be detected experimentally as a strong ligand

(15) Andersson, P. G.; Sharpless, K. B. *J. Am. Chem. Soc.* **1993**, *115*, 7047.

(16) Kolb, H. C.; Andersson, P. G.; Sharpless, K. B. *J. Am. Chem. Soc.* **1994**, *116*, 1278.

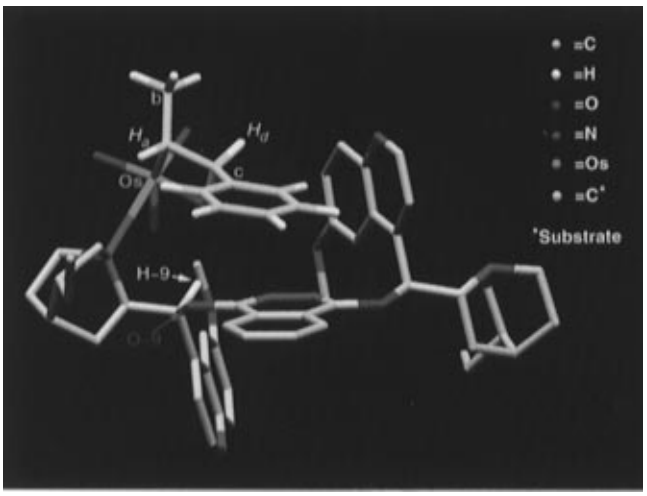

Figure 6. The predicted major intermediate in the dihydroxylation of *trans*-β-methylstyrene with $(DHQD)_2$-PHAL as ligand. It corresponds to **A** in Figure 3, **5** in Figure 5, and the top isomer in Figure 7. Carbons of the substrate are highlighted in yellow.

acceleration when complementary large groups are present at O-9 on the ligand and position **c** on the oxetane.[4e,16] In intermediate **B**, the conformation leading to attractive stabilization is much less accessible, due to a strong repulsive interaction between H_a in the oxetane and H-9 in the *cinchona*-derived ligand (*cf.* Figure 8).

Regioisomeric Oxetanes and Enantiofacial Selectivity. Even when the preferred path is through the particular conformer of diastereomer **A** shown in Figure 3 and position **a** on the oxetane is constrained to be hydrogen, different isomers of the oxetane can usually be formed for mono- and disubstituted olefins. Of course, symmetrical disubstituted olefins can yield only one isomeric complex under these constraints (types **5**, **6**, and **9**, Figure 5). The best enantioselectivity to date has been obtained with *trans*-stilbene, which under optimized conditions affords an ee of >99.8%; hence the pathway through isomer **A** is strongly dominant over the path through isomer **B**. Such good results are quite general for *trans*-disbustituted olefins (symmetric or unsymmetric), as well as for trisubstituted olefins which are also limited to one isomeric form under the constraints defined above. However, it should be noted that it is possible to design olefins with sterically demanding groups in position **c** that will not experience nonbonded stabilization in the molecular mechanics model. These are not expected to favor **A** over **B**, and indeed give low ee experimentally.[4g]

It is possible to gain information about the isomeric forms of the intermediate oxetane by studying the effects of different mono methyl substitutions on styrene (α- or β-methylstyrenes). The various methyl groups will be expected to curtail or block certain of the competing metallaoxetane paths, but they are not large enough to furnish the attractive nonbonded stabilization which is so essential for good selectivities in the AD reaction.[17] A consistent picture emerges upon comparing the enantioselectivities for dihydroxylation in the presence of *cinchona*-derived ligands.[18,2] The values are shown in Table 2.

Table 2. Enantioselectivities and Relative Rates Found in the AD Reaction on Substituted Styrenes in the Presence of Two Different Ligands

		DHQD-CLB			$(DHQD)_2$-PHAL		
entry	substrate	ee (%)	ref	rate[a]	ee (%)	ref	rate[a]
1	*trans*-β-methylstyrene	91	28	8	98	*b*	4
2	styrene	74	2c	1	97	2a	1
3	α-methylstyrene	62	20	0.8	94	2a	0.5
4	*cis*-β-methylstyrene	35	29	0.5	35	30	0.1

[a] Rate of dihydroxylation relative to styrene determined by competition experiments under stoichiometric conditions in *t*-BuOH/H_2O (6:1, the same ratio as in the organic phase in the catalytic AD) at 0 °C.[31] It should be noted that for all olefin classes, the rate of the background reaction (i.e., without ligand) is negligible. [b] This work.

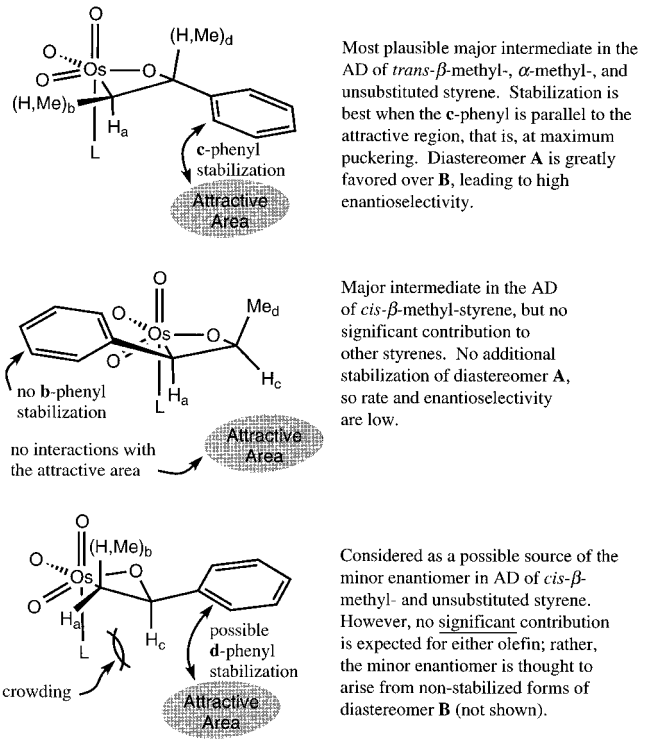

Figure 7. Possible isomeric forms of diastereomer **A**.

Starting with *trans*-β-methylstyrene, one notes that it is almost as good a substrate as stilbene (entry 1, Table 2). Two favored regioisomers of **A** are possible: **c**-phenyl, **b**-methyl or **b**-phenyl, **c**-methyl, and each is a precursor of the observed major enantiomer. The very high ee for stilbene clearly shows that both positions **b** and **c** can accommodate the phenyl group and that diastereomer **A** (giving (*R*,*R*)-diol) is substantially favored over **B** (giving (*S*,*S*)-diol). A phenyl group in position **c** experiences the experimentally observed nonbonded attraction from the O-9 substituent.[16] Figure 6 shows how the second generation PHAL-ligand encloses the **c**-substituent in diastereomer **A**, thereby achieving stabilization of the intermediate through several nonbonded interactions. In the molecular mechanics model, it has not been possible to find a conformation where a **b**-phenyl can experience similar stabilization, from either the aromatic O-9 substituent or the methoxyquinoline moiety, without at the same time causing strong repulsion in other parts of the molecule. These observations suggest that the reaction of *trans*-β-methylstyrene is channeled predominantly through the **c**-phenyl, **b**-methyl regioisomer of **A** (as in Figure 6; see also Figure 7, top).

(17) Vanhessche, K. P. M.; Sharpless, K. B. Unpublished results. See also ref 2f.

(18) Since 1987 a number of cinchona derivatives have been used, but for most of these ligands where a comparison has been made, the results for the methylstyrenes show similar trends; see ref 2.

(19) Kwong, H.-L.; Sorato, C.; Ogino, Y.; Chen, H.; Sharpless, K. B. *Tetrahedron Lett.* **1990**, *31*, 2999.

(20) Wang, L.; Sharpless, K. B. Unpublished results.

(21) Becker, H.; King, S. B.; Taniguchi, M.; Vanhessche, K. P. M.; Sharpless, K. B. *J. Org. Chem.* **1995**, *60*, 3940.

(22) Styrene is dihydroxylated about 7 times faster with $(DHQD)_2$-PHAL then with DHQD-CLB as ligand. It should be noted, that *all* olefins examined in this study are dihydroxylated faster by $(DHQD)_2$-PHAL than by DHQD-CLB (see ref 16).

The result for unsubstituted styrene with $(DHQD)_2$-PHAL is almost as good as that for *trans*-β-methylstyrene (entry 2, Table 2). It is clear that a phenyl group in position **c** still furnishes enough stabilization for diastereomer **A** to make contributions from diastereomer **B** of minor importance when the dimeric PHAL ligand is used. The result with DHQD-CLB is more interesting, revealing that an alternate pathway leading to the opposite enantiomer has been opened by the removal of the **b**-methyl group. For all arguments herein it is essential to realize that *both* major and minor enantiomers arise from ligand assisted pathways. The background reaction is too slow to make any contribution. There are two possible sources of the minor enantiomer: Either the path through diastereomer **B** becomes operative, or the phenyl group can occupy position **d** in diastereomer **A** (Figure 7, bottom). A **d**-phenyl might experience some attractive stabilization by the ligand if the puckering of the osmaoxetane is reversed. This ring flip would put the **d**-phenyl into a favorable pseudoequatorial position (i.e. position **d** in **8** with an H at position **a**). Such conformations could indeed be found in the molecular mechanics calculations and were found to experience reasonably high stabilization from nonbonded attractions. However, no energy minima corresponding to such a reversed puckering could be found for monosubstituted olefins in the DFT calculations (*vide supra*). The likely alternative is that the increased puckering of the osmaoxetane ring due to the presence of a **b**-methyl (*vide supra*) enhances the capacity of the **c**-phenyl to experience stabilization (Figure 7, top). In the absence of the **b**-methyl the energy difference between isomers **A** and **B** (the latter cannot experience stabilization) would decrease. Another possible explanation for a pathway through isomer **B** would be an electronic preference of position **b** for the phenyl group (Figure 7, middle). Despite the bulk of the phenyl group, position **b** could conceivably be favored due to the possibility of conjugation with the metal-bound carbon. As substituents in this position cannot experience nonbonded stabilization, **b**-phenyl isomers would be expected to lead to approximately equal amounts of the two enantiomers. However, a **b**-preference for the phenyl groups should be even more pronounced for *trans*-β-methylstyrene, since the methyl group should compete for the sterically favored position **c**. Since the ratio of enantiomers is 99:1, a maximum of 1% of the product in AD of *trans*-β-methylstyrene could arise from a **b**-phenyl-**B** isomer. This path should be even less favored for styrene, so we conclude that no significant amount of the product is formed from a **b**-phenyl isomer for the parent aromatic olefin.

With α-methylstyrene, only positions **c** and **d** can be used for the two substituents. The puckering of the osmaoxetane ring will decrease due to the presence of a pseudoaxial substituent in position **d**. However, reverse puckering to achieve stabilization of the **d** substituent is no longer possible due to strong repulsion between the **c** substituent and the quinuclidine moiety of the alkaloid (L and H_c, Figure 7, bottom). The enantioselectivity is still substantial, but lower than for both styrene and *trans*-β-methylstyrene. As no alternative, stabilized pathways are possible, these results suggest that the reduced puckering of the ring decreases the stabilization available to isomer **A** relative to that for styrene and *trans*-β-methylstyrene.

A drastic decrease in performance is observed with *cis*-β-methylstyrene. Both the observed enantioselectivity and the reaction rate are decreased for *cis*-disubstituted olefins compared to all other olefin classes. This is readily explained by the model, as position **c** cannot be used for the phenyl substituent since it places a methyl group in the congested **a** position. In the absence of this stabilization, isomer **A** is no longer strongly

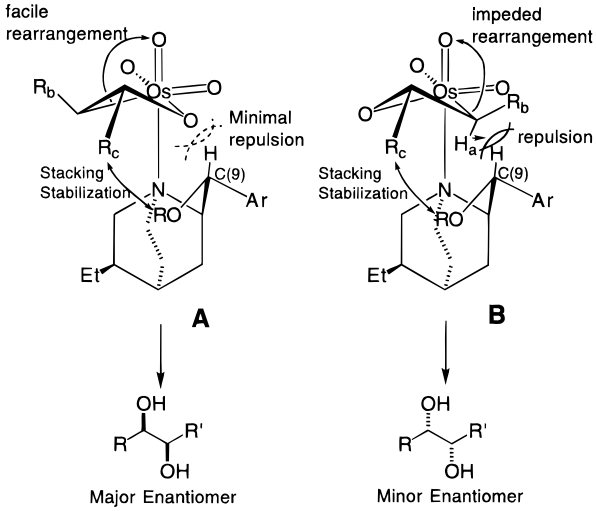

Figure 8. Steric effects on the rearrangement of the intermediate.

favored over **B**, because in either case the two substituents will be in the **b** and **d** positions, where no strong interactions, attractive or repulsive, exist. Since position **b** is still accessible to the phenyl group, if stabilization of a **b** substituent was possible, *cis*-β-substituted styrenes would be expected to show enantioselectivities comparable to, for example, styrene itself. This lends additional support to the hypothesis that styrene and *trans*-β-methylstyrene preferentially react via the pathway where their phenyl group resides in position **c**. The configuration at the benzylic carbon for the major enantiomer from *cis*-β-methylstyrene is the same as for the other styrenes (*R* with DHQD-derived ligands), and this excludes the possibility of significant stabilization for a **d**-phenyl-**A** isomer, as this would lead to the opposite enantiomer (Figure 7, bottom). In summary, for *cis*-β-methyl styrene, diastereomer **A** again seems preferred, but with the phenyl group now in position **b** (Figure 7, middle). An alternative path leading to the observed major product that involves reaction through **d**-phenyl-**b**-methyl-**B** is less probable (*vide infra*).

The low enantioselectivity and rate observed for *cis*-1,2-disubstituted olefins indicates that several paths, all with high activation barriers, are open to this class of olefins. In fact, it cannot be excluded that *cis*-olefins react in a manner similar to tetrasubstituted olefins, that is with the two substituents allowed in positions **a** and **c**. The *transition state*, not an intermediate, would then resemble structure **7**. This would allow some stabilization of a **c**-substituent in a manner analogous to that discussed previously for the more favorable olefin classes. It may be possible to test the importance of this alternate pathway by studying the effect of varying the size of the aromatic moiety, in analogy with the preceding kinetic study of monosubstituted olefins.[16]

The puckering of the osmaoxetane also affects the rearrangement of the oxetane to the glycolate. As shown in Figure 8, the rearrangement of the diastereomeric oxetane **A** (see also Figure 3) proceeds without major steric impediments. From tentative modeling studies, it also seems reasonable to assume that the attractive stabilization is even more pronounced in the rearrangement transition state than in the intermediate. In **B** however, a severe repulsive interaction occurring between H_a and H-C(9) will interfere with the rearrangement in addition to the previously recognized effect of lowering the steady state concentration of isomer **B**.[4e] This unfavorable interaction is stronger for the more puckered *trans*-1,2-disubstituted olefins because H_a and H-C(9) come closer than in the less puckered monosubstituted cases. This *second level* of selection adds

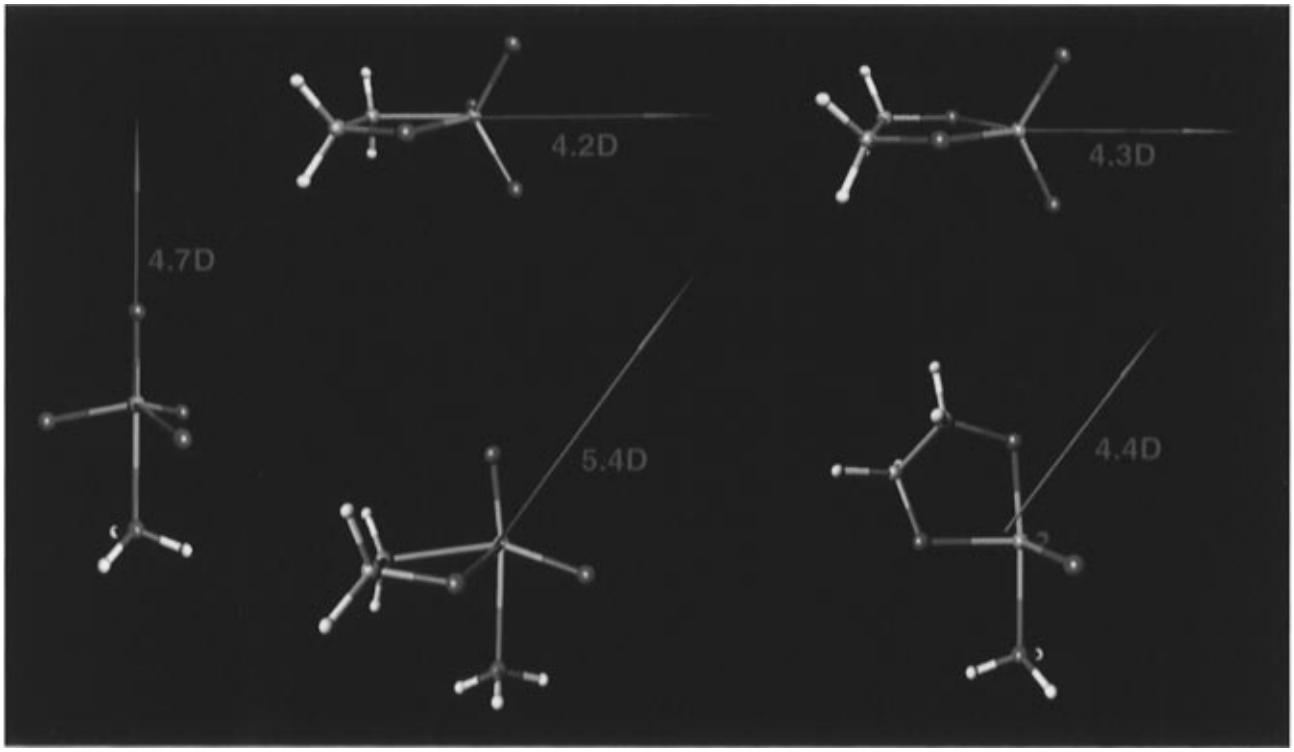

Figure 9. Dipole moments of selected ruthenium species (in Debye). The ligand is ammonia in all cases.

another possible rationalization for the correlation between ring puckering and enantioselectivity.

The preceding analysis has focused on the importance of the nonbonded attractive stabilization in the AD reaction. It is certainly true that the best results are obtained when an aromatic or a properly shaped aliphatic group is present to direct the olefin into the preferred orientation. However, even in the absence of stabilizing interactions, the AD reaction still yields enantiomerically enriched product, and more importantly, with the same substituent trends and face selectivity as for substrates which can experience stabilizing interactions. Thus, the AD of propene in the presence of the $(DHQD)_2$-PHAL ligand gives (*R*)-propylene glycol with an ee of 36%, whereas *trans*-2-butene with the same ligand gives an ee of 72%.[2f] It can therefore be concluded that intermediate **A** is stabilized over **B** even in the absence of large groups in position **c** on the oxetane. Furthermore, even when the size of the O-9 substituent is drastically reduced, enantioselection is still observed. For example, AD of propene in the presence of DHQD-acetate still yields 20% ee, down from 36% ee for $(DHQD)_2$-PHAL under the same conditions.

A possible explanation for this residual (i.e. after large effects are stripped away) enantioselectivity contribution is a favorable dipole−dipole interaction between the ligated osmaoxetane and the ester/iminoester moiety of the ligand. Examination of the electrostatic environment reveals that the dipoles of the metallaoxetane and the O9-substituent in diastereomer **A** (but not **B**) are oriented approximately antiparallel, perhaps leading to additional stabilization of the intermediate. The dipole moment of the ligated oxetane is the largest found in a series of ruthenium structures calculated (Figure 9). The large dipole (5.4 D) for this key intermediate is also consonant with the observed solvent effects in the AD: addition of nonpolar cosolvents (*e.g.* toluene in place of *t*-BuOH) usually produces severe drops in both enantioselectivity and rate.[16]

Finally, an additional small contribution to the enantioselectivity may be attached to the skewing (twisting) of the quinuclidine moiety of the ligand. The DHQD-ligands have a strong skewing and in most cases give higher enantioselectivity than the corresponding DHQ-ligands, which are twisted in the mirror image sense, but only slightly.[23] For example, propene yields 15% ee with DHQ-acetate as ligand, whereas the reaction with DHQD-acetate proceeds with 20% ee.

Computational Details. All DFT calculations have been performed on a Cray Y-MP computer using the UniChem DGauss 1.1.1 program.[24] The DZVP basis set supplied with the program has been used for all atoms. The Becke−Perdew nonlocal correction was applied self-consistently.

Experimental Section

For general experimental procedures see lit.[25] The ligands DHQD-acetate and DHQ-acetate were prepared as described in the literature.[4b,26]

(1*R*,2*R*)-1-Phenylpropane-1,2-diol. The AD of *trans*-β-methylstyrene was performed using the standard conditions described in ref 2a on 1 mmol scale; (1*R*,2*R*)-1-phenylpropane-1,2-diol was obtained in 80% yield. The ee was determined to be 98% by HPLC analysis of the diol (Chiralcel AD, 10% *i*-PrOH/hexane, 0.5 mL/min, 254 nm; 12.3 min (*S*), 18.0 min (*R*)). $[\alpha] = -31.7$ ($c = 0.99$, EtOH); ^{1}H NMR ($CDCl_3$, 400 MHz) δ 7.38−7.29 (m, 5H); 4.39 (dd, $J = 7.4$, 3.3, 1 H); 3.91−3.83 (m, 1 H); 2.57 (d, $J = 3.3$, 1 H); 2.43 (d, $J = 3.4$, 1 H); 1.07 (d, $J = 6.3$, 3 H); ^{13}C NMR ($CDCl_3$, 100 MHz) δ 141.0, 128.4, 128.1, 126.8, 79.4, 72.2, 18.7; MS (FAB^+/NBA/NaI) calculated for $C_9H_{12}O_2$ (MNa^+), 175.0735, found, 175.0739.

(*R*)-Propane-1,2-diol. $K_3Fe(CN)_6$ (5.00 g, 15 mmol), K_2CO_3 (2.07 g, 15 mmol), $K_2OsO_2(OH)_4$ (14.5 mg, 0.04 mmol), and dihydroquinidine-acetate (37 mg, 0.1 mmol) were dissolved in 50 mL of 1:1 *t*-BuOH/H_2O. The mixture was cooled to 0 °C and a slow stream of propene bubbled through. The reaction was quenched after 18 h by addition of 3 g of Na_2SO_3. It was warmed to room temperature and stirred for

(23) Dijkstra, G. D. H.; Kellog, R. M.; Wynberg, H.; Svendsen, J. S.; Markó, I.; Sharpless, K. B. *J. Am. Chem. Soc.* **1989**, *111*, 8069.
(24) DGauss 1.1.1, part of UniChem 1.1.1 from Cray Research, Inc.
(25) Becker, H.; Soler, M. A.; Sharpless, K. B. *Tetrahedron* **1995**, *51*, 1345.
(26) (a) Hesse, O. *Justus Liebigs Ann. Chem.* **1887**, *241*, 255. (b) Hesse, O. *Justus Liebigs Ann. Chem.* **1882**, *214*, 1.

30 min. The mixture was extracted 4 times with 50 mL of ethyl acetate; the combined organic layers were dried with $MgSO_4$, the solvent was evaporated, and the residue was purified by distillation in a kugelrohr (1 mmHg, 120 °C). (*R*)-Propane-1,2-diol (347 mg, 4.56 mmol, 61% based on $K_3Fe(CN)_6$) was obtained as a colorless oil; the ee was determined to be 20% (*vide infra*). $[\alpha] = -5.0$ ($c = 1.12$, H_2O); ^{1}H NMR ($CDCl_3$, 400 MHz) δ 3.93−3.86 (m, 1 H), 3.61 (dd, $J = 11.2$, 3.0 Hz, 1 H); 3.39 (dd, $J = 11.2$, 7.9 Hz, 1 H); 3.09 (s, br, 2H); 1.15 (d, $J = 6.3$, 3 H);

The absolute configuration was assigned by comparison of the optical rotation with the literature value.[27] To determine the ee, propane-1,2-diol was converted to the bis(*p*-methoxy benzoate) (*vide infra*).

A similar reaction with dihydroquinine-acetate as ligand furnished (*S*)-propane-1,2-diol in 15% ee (59% yield based on $K_3Fe(CN)_6$); $[\alpha] = +3.8$ ($c = 0.97$, H_2O).

(*R*)-1,2-Bis[(*p*-methoxybenzoyl)oxy]propane. (*R*)-Propane-1,2-diol (5 mg, 0.066 mmol) (20% ee) was dissolved in 2 mL of dry CH_2Cl_2. 4-(Dimethylamino)pyridine (33 mg, 0.26 mmol) and 34 mg (0.20 mmol) of *p*-anisoyl chloride (distilled) were added at room temperature. After stirring for 1 h, 5 mL of CH_2Cl_2 was added; it was washed with 5 mL of saturated aqueous NH_4Cl solution and with 5 mL of saturated aqueous $NaHCO_3$ solution. The organic phase was dried by filtration through cotton. Flash chromatography (SiO_2, 4:1 hexane/ethyl acetate) furnished 20 mg (0.057 mmol, 86%) of (*R*)-1,2-bis[(*p*-methoxybenzoyl)-oxy]propane as a colorless oil. The ee was determined by HPLC (Chiralcel OD-H, 10% *i*-PrOH/hexane, 1 mL/min, 254 nm; 11.9 min (*R*), 16.0 min (*S*)). $[\alpha] = +7.3$ ($c = 1.30$, $CHCl_3$); ^{1}H NMR ($CDCl_3$, 400 MHz) δ 8.02−7.95 (m, 4 H), 6.93−6.87 (m, 4 H), 5.52−5.47 (m, 1 H), 4.45 (d, $J = 4.8$, 2 H), 3.86 (s, 3 H), 3.84 (s, 3 H), 1.45 (d, $J = 6.5$, 3 H); ^{13}C NMR ($CDCl_3$, 100 MHz) δ 165.8, 165.5, 163.3, 163.2, 131.6, 131.5, 122.5, 122.1, 113.5, 113.4, 68.5, 66.3, 55.2, 16.6; MS (FAB^+/NBA/CsI) calculated for $C_{19}H_{20}O_6$ (MH^+), 345.1338; found, 345.1353.

Determination of the Relative Rates for Styrene, α-Methylstyrene, *trans*-β-Methylstyrene, and *cis*-β-Methylstyrene. Styrene (4 mmol), α-methylstyrene (4 mmol), *trans*-β-methylstyrene (4 mmol), and *cis*-β-methylstyrene (4 mmol) and ligand (0.50 mmol, 390 mg in the case of $(DHQD)_2$-PHAL, 232.5 mg in the case of DHQD-CLB) were dissolved in 80 mL of 6:1 *t*-BuOH/H_2O and cooled to 0 °C. Under vigorous stirring a solution of OsO_4 (50.8 mg, 0.20 mmol) in 1.25 mL 6:1 *t*-BuOH/H_2O was added dropwise over a period of 1 h. The green solution was stirred for additional 3 h. A slow stream of H_2S was bubbled through for 30 min. Then N_2 was bubbled through the black reaction mixture for 30 min. The mixture was filtered through Celite and the solvent was evaporated. The residue was filtered through a 1 cm × 15 cm plug of silica (hexane + 10% ethyl acetate until all remaining olefins were eluted and then 1:1 hexane/ethyl acetate and 1:2 hexane/ethyl acetate). The product composition is determined by integration of the following ^{1}H NMR signals (CD_3OD, 400 MHz): 4.68 (dd, $J = 7.1$, 5.1 Hz, 1H; styrenediol); 4.50 (d, $J = 5.2$ Hz, 1H, *cis*-β-methylstyrenediol); 4.33 (d, $J = 7.1$ Hz, 1H, *trans*-β-methylstyrene-diol); 1.50 (s, 3H, α-methylstyrenediol); 1.11 (d, $J = 6.4$ Hz, 3H, *cis*-β-methylstyrenediol); 0.95 (d, $J = 6.4$ Hz, 3H, *trans*-β-methylstyrenediol). The composition of the product represents the relative rates (see Table 2) of the olefins used in this study.

Acknowledgment. We are grateful to Professor K. Gable for penetrating insights and to Dr. S. Loren for valuable discussions about nonbonded interactions. P.O.N. thanks the Danish Medical Research Council and the Trygger foundation for support. H.B. thanks the *Fond der Chemischen Industrie* for a fellowship. We thank the National Institute of Health (GM 28384) and the National Science Foundation (CHE-9296055) for financial support.

Supporting Information Available: Structural details, including selected bond lengths and torsion angles, for the calculated metallaoxetane ligand complexes **1**−**10** (1 page). This material is contained in many libraries on microfiche, immediately follows this article in the microfilm version of the journal, can be ordered from the ACS, and can be downloaded from the Internet; see any current masthead page for ordering information and Internet access instructions.

JA952470C

(27) Huff, E. *Biochim. Biophys. Acta* **1961**, *48*, 506.